Published in final edited form as:
Neurosci Lett. 2011 July 25; 499(3): 143–148. doi:10.1016/j.neulet.2011.05.056.

OLIGODENDROCYTE VULNERABILITY FOLLOWING TRAUMATIC BRAIN INJURY IN RATS

George Lotocki, PhD[2], **Juan de Rivero Vaccari, PhD**[1,2], **Ofelia Alonso, BS**[2], **Juliana Sanchez Molano, MD**[2], **Ryan Nixon**[2], **Padideh Safavi**[2], **W. Dalton Dietrich, PhD**[1,2], and **Helen M. Bramlett, PhD**[1,2,3]

[1]Department of Neurological Surgery, University of Miami Miller School of Medicine, Miami, FL

[2]The Miami Project to Cure Paralysis, University of Miami Miller School of Medicine, Miami, FL

[3]Bruce W. Carter Department of Veterans Affairs, Medical Center, Miami, Florida, USA

Abstract

Experimental and clinical findings demonstrate that traumatic brain injury (TBI) results in injury to both gray and white matter structures. The purpose of this study was to document patterns of oligodendrocyte vulnerability to TBI. Sprague Dawley rats underwent sham operated procedures or moderate fluid percussion brain injury. Animals were perfusion-fixed for quantitative immunohistochemical analysis at 3 (n=9) or 7 (n=9) days post-surgery. Within the ipsilateral external capsule and corpus callosum, numbers of APC-CC1 immunoreactive oligodendrocytes were significantly decreased at 3 or 7 days post-TBI compared to sham rats ($p<0.03$). At both posttraumatic survival periods, double-labeling studies indicated that oligodendrocytes showed increased Caspase 3 activation compared to sham. These data demonstrate regional patterns of oligodendrocyte vulnerability after TBI and that oligodendrocyte cell loss may be due to Caspase 3-mediated cell death mechanisms. Further studies are needed to test therapeutic interventions that prevent trauma-induced oligodendrocyte cell death, subsequent demyelination and circuit dysfunction.

Keywords

myelin; oligodendrocyte; apoptosis; brain trauma

INTRODUCTION

Traumatic brain injury (TBI) is a devastating injury that can lead to long term paralysis, severe deficits in learning and memory and posttraumatic epilepsy [23, 25]. The neuropathological consequences of brain trauma consist of a wide range of structural changes [13, 17]. To investigate the pathophysiological consequences underlying the vulnerability of the brain to trauma, clinically relevant animal models have been developed [8, 11]. These models have provided a rich literature on the structural and behavioral changes observed following TBI (for review see [2, 6]).

Diffuse/traumatic axonal injury (DAI/TAI) is a common consequence of clinical and experimental TBI [5, 14, 27, 28]. Clinical studies have concluded that axonal damage may be a major mechanism underlying the functional consequences of TBI [14, 15]. The regional

Correspondence to: Helen M. Bramlett, Ph.D., Department of Neurological Surgery, University of Miami Miller School of Medicine, 1095 NW 14th Terrace, LPLC 3-18, Miami, FL 33136-1060, 1-305-243-8926 (work), 1-305-243-3914 (fax), hbramlett@miami.edu.

and temporal profile of axonal damage have been described in both focal and diffuse models of TBI [5, 27, 28]. Other studies have documented some evidence of myelin disruption after TBI and death of oligodendrocytes [4, 7, 29, 32]. However, the regional and temporal profile of oligodendrocyte vulnerability in a reproducible model of TBI has not been described. Such data would be important because in addition to primary axonal damage, damage to oligodendrocytes and subsequent demyelination would be expected to impair the ability of white matter tracts to effectively communicate in a highly orchestrated manner [12].

Recent studies have emphasized the progressive nature of gray and white matter vulnerability after TBI [4, 11, 26]. Bramlett and colleagues [5] first reported that rats living months after TBI showed widespread evidence of atrophy within cortical and subcortical areas. In clinical studies, atrophy of white matter tracts and subsequent demyelination is a common occurrence in patients with chronic TBI. The major purpose of this study was to quantitatively assess oligodendrocyte cell death after moderate fluid percussion brain injury using APC-CC1, a specific marker for oligodendrocytes, [1, 24] and the activated form of Caspase 3.

MATERIALS AND METHODS

Fluid Percussion Brain Injury

Male Sprague-Dawley rats (270–380 gms; Charles River Laboratories) received TBI using the moderate parasagittal fluid percussion (FP) injury model that results in neuropathological and behavioral consequences [33]. All experimental procedures were in compliance with the *Guide for the Care and Use of Laboratory Animals* and approved by the University of Miami Animal Care and Use Committee. One day prior to TBI, animals were randomly assigned to either the sham (n=6) or TBI (n=12) group and then anesthetized with 3% isoflurane, 70/30% N_2O/O_2 and received a 4.8-mm craniotomy (3.8 mm posterior to bregma, 2.5 mm lateral to the midline) to anchor a modified plastic 18-gage syringe hub (8 mm length; Becton Dickinson) over the exposed dura of the right parietal cortex. Twenty-four hours after the craniotomy, animals were anesthetized with 3% isoflurane, 70/30% N_2O/O_2 then intubated endotracheally and mechanically ventilated (Harvard Apparatus) with 1.5% isoflurane, 70/30% N_2O/O_2. To facilitate mechanical ventilation, Pancuronium Bromide (0.5 mg/kg) was intravenously administered. The femoral artery was cannulated to monitor blood gases (PO_2 and PCO_2), pH and mean arterial blood pressure (MABP) which were maintained within normal physiological range at 15 minutes before TBI and up to four hours after TBI.

Sham and TBI animals were attached to the FP device and the TBI animals received a moderate FP pulse (2.0 ± 0.2 atmospheres) delivered to the right parietal cortex. Sham operated animals underwent all surgical procedures except for the FP pulse. Rectal and temporalis muscle thermistors measured core and brain temperatures respectively using self-adjusting feedback warming lamps. There were no complications throughout the experiments so that no animals were lost due to injury or post-surgical processing of tissue.

Immunohistochemical Analysis

At 3 (n=9) or 7 days (n=9) after TBI or sham procedures, animals were anesthetized using 3% isoflurane, 70/30% N_2O/O_2 and transcardially perfused with saline then with 4% paraformaldehyde in phosphate-buffered saline (PBS). The brains were sectioned in PBS (60 μm thick) with a Leica Vibratome or Leica SM2000R (Leica Microsystems, Inc., Exton, PA, U.S.A.) from bregma levels −2.3mm to −5.8mm. Free-floating sections were blocked for one hour at room temperature in blocking buffer (PBS containing 5% normal goat serum, and 0.3% TX-100). Sections were incubated overnight in 4°C in blocking buffer containing

primary antibodies, rinsed with PBS and incubated for two hours at room temperature in blocking buffer containing secondary antibodies. The sections were rinsed with PBS and mounted using Prolong Gold Anti-Fade Mounting Medium (Invitrogen, Carlsbad, CA, U.S.A.). Primary antibodies used were mouse anti-APC-CC1, against adenomatous polyposis coli gene, mIgG (1:500; Calbiochem; [1], activated form of rabbit anti-Caspase 3 (1:500; Millipore; AB3623), rabbit GFAP (1:500; Millipore; AB5804). Controls lacking the primary antibody were run in parallel to evaluate the potential for non-specific labeling. Secondary antibodies used were Alexa 488-, 546- labeled anti-rabbit and anti-mouse antibodies (Invitrogen) for confocal analysis or biotinylated antibodies (1:250; Vector Laboratories) followed by diaminobenzidine (DAB) for stereological assessment [22].

The external capsule and corpus callosum were quantitatively assessed using a non-biased stereological approach to cell counting [33] by a blinded observer. Images were obtained by montaging Y-field epiflourescent 40X magnification images using Neurolucida 7.5.1 software (Micro-Bright Field Inc., Williston, VT, U.S.A.). Higher magnification optical imaging was performed using a LSM510 laser scanning confocal microscope (Carl Zeiss, Inc., Thromwood, N.Y., U.S.A.) using 25X 0.8 ma and 63X 1.2 ma water-immersion lenses. To minimize experimental variability, sections from each experimental group were processed in parallel and imaged during the same imaging session using identical microscope settings and the final images were scaled identically. Five specific bregma levels (−2.8, −3.3, −3.8, −4.3, −4.8mm) were selected for each animal. For region of interest analysis and oligodendrocyte cell counts, specific anatomical landmarks were used to define the boundaries of each structure. These boundaries were based on previous histopathological studies indicating regions of hemorrhagic contusion formation, selective cortical neuronal vulnerability and white matter damage as assessed by β-amyloid precursor protein immunoreactivity [33].

Stereology

The number of APC-CC1 positive cells was quantified in the external capsule and corpus callosum by a blinded observer. Serial sections (60 μm) of the rat brain at the level of injury were divided into 5 groups; each group contained 5 sections representing areas containing the contusion as well as regions rostral and caudal. For estimation of the number of APC-CC1 immunopositive cells, DAB was used as the chromagen. White matter tract regions in animals at 3 and 7 days after TBI were analyzed using an Axiophot (Zeiss, Inc.) research microscope, furnished with a fully motorized 3-D LEP stage, Optronix cooled video camera, and MicroBrightField Inc. Stereo-Investigator software package. Cell numbers were estimated using the optical fractionator method and optical dissector probe. Dimension of the optical dissector was designed based upon the cell distribution on the section, and optical fractionator grid size was determined based upon the results of the preliminary count of the naïve brain sample to allow 200 counts per brain region. Immunoreactive cells were those that had degrees of cell body stain greater than controls lacking primary antibody. In addition, positive oligodendrocytes were identified by their morphology as ameboid in shape compared to any potential cross-reactivity with CC1 positive astrocytes as previously described [1].

Five sections between bregma levels −3.3 and −4.3 mm were chosen for stereological analysis. Bregma levels were identical in all animal groups and primarily focused at the area surrounding the epicenter of the injury (bregma level −3.8 mm). A counting grid 150 × 150 um was placed over the corpus callosum and external capsule on the ipsilateral side of the injury. For sections immunostained with anti-CC-1, the section thickness was 30 um and the optical dissector height was 20 um with 5 um guard zones. Using a 30 × 30 um counting frame CC-1-positive cells were counted in 27–61 randomly-placed sampling sites with a 63×, 1.42 NA objective. For CC-1 immunoreactive cell counts in the corpus callosum *Q*

values range was 300–730, and CE^2/CV^2 values were 0.29, 0.23, 0.50, 0.45 for the 3 day sham, 7 day sham, 3 day post TBI, 7 day post TBI groups respectively. For CC-1 immunoreactive cell counts in the external capsule Q values range was 171–528, and CE^2/CV^2 values were 0.21, 0.29, 0.59, 0.15 for the 3 day sham, 7 day sham, 3 day post TBI, 7 day post TBI groups respectively. Images were taken with 1×, 10× and 20× objectives on a BX51TRF microscope (Olympus America).

Statistical Analysis

Data presented are mean ± SEM. Physiological data were analyzed using one-way repeated measures analysis of variance followed by post hoc analysis (Fisher LSD). Cell count data were analyzed using t-tests comparing 3 and 7 day outcome to control, $p<0.025$ due to multiple comparisons within each structure (Bonferroni correction).

RESULTS

Physiological Variables

All physiological variables (pH, PO_2, PCO_2, and MABP) were within normal ranges prior to and following the traumatic insult. No significant differences were seen between any of the experimental groups (data not shown).

Immunocytochemistry

Sham-operated animals (n=6) showed a high frequency of CC1 immunoreactive cells within both gray and white matter structures. CC1 immunoreactive cells were localized in white matter tracts including the corpus callosum and external capsule (Figure 1A–C). For example, immunoreactive cells were commonly lined up in rows parallel to the projecting axonal fibers.

At three (n=6) and seven (n=6) days after traumatic brain injury, there was an observable reduction in the number of CC1-positive cells within the external capsule (Figure 1D–F). At the site of contusion, along the gray-white interface for example, there was a lack of stained cells within the evolving contusion site (Figure 1D,E). Also, in the corpus callosum, there was a visible reduction in the number of immunoreactive cells compared to sham (Figure 1D,F).

Previous reports [1] utilizing CC1 as an immunomarker for oligodendrocytes have demonstrated that CC1 clearly stains oligodendrocytes with other cell types such as astrocytes and Schwann cells only weakly stained. In Figure 2, we observed a lack of double-stained CC1 oligodendrocytes (red) and GFAP positive astrocytes (GFAP) within the corpus callosum, and external capsule following TBI. Therefore, the combination of CC1 as a marker for oligodendrocytes and established morphological parameters allowed us to identify oligodendrocytes for quantitative assessment.

Caspase 3 Immunoreactivity

To determine whether oligodendrocytes express activated Caspase 3 after TBI, double-labeling studies were conducted. Vibratome sections were double-stained with APC-CC1 and activated Caspase 3. In contrast to sham-operated animals, a high frequency of double-labeled cells were seen within the cerebral cortex at three (Figure 3) and seven days after TBI. These double-stained cells were scattered among other cells that were only CC1 immunoreactive. These data indicate that oligodendrocytes in vulnerable brain regions appear to be undergoing apoptotic cell death by Caspase 3 mediated mechanisms.

Quantitative Analysis

Non-biased cell counting approaches in sham operated animals demonstrated a consistent number of immunoreactive oligodendrocytes within the external capsule and corpus callosum. No significant differences were observed between sham animals at 3 (n=3) and 7 (n=3) days so both groups were combined for comparison to the TBI groups. At both three days (n=6) and seven (n=6) days after TBI, reductions in the number of immunoreactive oligodendrocytes were seen in all structures analyzed (Figure 4). T-test was significant ($p<0.001$) for both time points compared to sham for the corpus callosum. For example, robust reductions in immunoreactive cell numbers were seen within the corpus callosum at 3 ($p<0.001$) and 7 ($p<0.001$) days post-injury compared to sham (Figure 4B). Within the external capsule, a significant ($p<0.02$) reduction in CC1 positive cells was seen at three days after injury compared to sham (Figure 4C). These data demonstrate the vulnerability of this cell population within affected brain regions after moderate traumatic brain injury.

DISCUSSION

In this study, we report that moderate FP brain injury leads to regional patterns of oligodendrocyte cell loss in white matter structures. Results show that at three and seven days after TBI, there are significant reductions in the frequency of CC1 immunoreactive oligodendrocytes in white matter tracts ipsilateral to the traumatic insult. These results show that oligodendrocytes are vulnerable to experimentally induced TBI.

Oligodendrocytes play an important role in the function of the central nervous system by enhancing conduction velocity down the axon fiber. For example, changes in the integrity of myelin insulation have been shown to lead to cognitive decline associated with aging and in patients with multiple sclerosis [16, 19]. The present studies are important in that they demonstrate patterns of oligodendrocyte vulnerability after TBI that could participate in the well-described behavioral consequences of this insult. Therapeutic interventions that reduce oligodendrocyte cell death or dysfunction may provide an important strategy to promote functional recovery after TBI.

Previous studies have investigated the potential pathomechanisms underlying oligodendrocyte cell death following a hypoxic/ischemic or traumatic insult [9, 10, 30, 31]. Following TBI, studies have reported that oligodendrocyte cells in the subcortical white matter undergo apoptotic cell death [7, 29, 32]. In a study by Shaw and colleagues [32], TUNEL-positive cells were identified in gray and white matter structures in specimens taken from head-injured patients that survived five hours to ten days after injury. Raghupathi and colleagues [29] reported a decrease in cellular Bcl-2 staining in some apoptotic-appearing TUNEL-positive cells within both gray and white matter structures.

Using the present model of FP brain injury, previous studies have characterized the cellular responses to injury [8]. In terms of potential mechanisms of neuronal cell death, Keane and colleagues [18] reported evidence for Caspase 3 immunoreactive cells throughout the traumatized hemisphere as early as 6 hours after TBI. In that study, some oligodendrocytes appeared to express Caspase 3. In the present study, we demonstrated that oligodendrocytes in white matter structures at three or seven days after TBI were immunoreactive for activated Caspase 3. Taken together, these studies are consistent with published data indicating that oligodendrocytes may die by apoptotic mechanisms following TBI.

Previous studies have reported that significant degrees of atrophy of both gray and white matter structures occur in this trauma model months and years after the injury (for review see [3]). Based on the present findings, future studies are required to determine whether

demyelination in this model occurs as a primary result of oligodendrocyte cell death and/or secondarily to Wallerian degeneration.

The current findings demonstrate oligodendrocyte vulnerability to moderate FP brain injury emphasizing this potentially significant consequence of TBI. In clinical conditions where abnormalities in myelination occur, different degrees of abnormal mental function have been described [12]. Following TBI, many behavioral abnormalities have been proposed to result from death of vulnerable neuronal populations, DAI, as well as a variety of posttraumatic injury mechanisms leading to circuit dysfunction and brain damage. Recent studies using diffusion tensor imaging have emphasized the complexity of white matter regions and relationships to cognitive ability [20, 21]. The present studies indicate that oligodendrocyte vulnerability and subsequent demyelination may be another mechanism underlying abnormal brain function after TBI. Therapeutic strategies that target oligodendrocyte vulnerability or promote oligodendrocyte genesis after TBI may represent an exciting therapeutic target for future interventions.

Acknowledgments

This work was supported by NS030291 and NS042133.

REFERENCES

1. Bhat RV, Axt KJ, Fosnaugh JS, Smith KJ, Johnson KA, Hill DE, Kinzler KW, Baraban JM. Expression of the APC tumor suppressor protein in oligodendroglia. Glia. 1996; 17:169–174. [PubMed: 8776583]
2. Bramlett HM, Dietrich WD. Pathophysiology of cerebral ischemia and brain trauma: similarities and differences. J Cereb Blood Flow Metab. 2004; 24:133–150. [PubMed: 14747740]
3. Bramlett HM, Dietrich WD. Progressive damage after brain and spinal cord injury: pathomechanisms and treatment strategies. Prog Brain Res. 2007; 161:125–141. [PubMed: 17618974]
4. Bramlett HM, Dietrich WD. Quantitative structural changes in white and gray matter 1 year following traumatic brain injury in rats. Acta Neuropathol (Berl). 2002; 103:607–614. [PubMed: 12012093]
5. Bramlett HM, Kraydieh S, Green EJ, Dietrich WD. Temporal and regional patterns of axonal damage following traumatic brain injury: a beta-amyloid precursor protein immunocytochemical study in rats. J Neuropathol Exp Neurol. 1997; 56:1132–1141. [PubMed: 9329457]
6. Cernak I. Animal models of head trauma. NeuroRx. 2005; 2:410–422. [PubMed: 16389305]
7. Conti AC, Raghupathi R, Trojanowski JQ, McIntosh TK. Experimental brain injury induces regionally distinct apoptosis during the acute and delayed post-traumatic period. J Neurosci. 1998; 18:5663–5672. [PubMed: 9671657]
8. Cortez SC, McIntosh TK, Noble LJ. Experimental fluid percussion brain injury: vascular disruption and neuronal and glial alterations. Brain Res. 1989; 482:271–282. [PubMed: 2706487]
9. Crowe MJ, Bresnahan JC, Shuman SL, Masters JN, Beattie MS. Apoptosis and delayed degeneration after spinal cord injury in rats and monkeys. Nat Med. 1997; 3:73–76. [PubMed: 8986744]
10. Dewar D, Underhill SM, Goldberg MP. Oligodendrocytes and ischemic brain injury. J Cereb Blood Flow Metab. 2003; 23:263–274. [PubMed: 12621301]
11. Dixon CE, Kochanek PM, Yan HQ, Schiding JK, Griffith RG, Baum E, Marion DW, DeKosky ST. One-year study of spatial memory performance, brain morphology, and cholinergic markers after moderate controlled cortical impact in rats. J Neurotrauma. 1999; 16:109–122. [PubMed: 10098956]
12. Fields RD. White matter in learning, cognition and psychiatric disorders. Trends Neurosci. 2008; 31:361–370. [PubMed: 18538868]

13. Gennarelli TA, Graham DI. Neuropathology of the Head Injuries. Seminars in clinical neuropsychiatry. 1998; 3:160–175. [PubMed: 10085204]

14. Gennarelli TA, Thibault LE, Adams JH, Graham DI, Thompson CJ, Marcincin RP. Diffuse axonal injury and traumatic coma in the primate. Ann Neurol. 1982; 12:564–574. [PubMed: 7159060]

15. Gentleman SM, Roberts GW, Gennarelli TA, Maxwell WL, Adams JH, Kerr S, Graham DI. Axonal injury: a universal consequence of fatal closed head injury? Acta Neuropathol (Berl). 1995; 89:537–543. [PubMed: 7676809]

16. Gootjes L, Teipel SJ, Zebuhr Y, Schwarz R, Leinsinger G, Scheltens P, Moller HJ, Hampel H. Regional distribution of white matter hyperintensities in vascular dementia, Alzheimer's disease and healthy aging. Dementia and geriatric cognitive disorders. 2004; 18:180–188. [PubMed: 15211074]

17. Graham DI, Raghupathi R, Saatman KE, Meaney D, McIntosh TK. Tissue tears in the white matter after lateral fluid percussion brain injury in the rat: relevance to human brain injury. Acta Neuropathol (Berl). 2000; 99:117–124. [PubMed: 10672317]

18. Keane RW, Kraydieh S, Lotocki G, Alonso OF, Aldana P, Dietrich WD. Apoptotic and antiapoptotic mechanisms after traumatic brain injury. J Cereb Blood Flow Metab. 2001; 21:1189–1198. [PubMed: 11598496]

19. Kujala P, Portin R, Ruutiainen J. The progress of cognitive decline in multiple sclerosis. A controlled 3-year follow-up. Brain. 1997; 120(Pt 2):289–297. [PubMed: 9117376]

20. Kumar R, Husain M, Gupta RK, Hasan KM, Haris M, Agarwal AK, Pandey CM, Narayana PA. Serial changes in the white matter diffusion tensor imaging metrics in moderate traumatic brain injury and correlation with neuro-cognitive function. J Neurotrauma. 2009; 26:481–495. [PubMed: 19196176]

21. Lo C, Shifteh K, Gold T, Bello JA, Lipton ML. Diffusion tensor imaging abnormalities in patients with mild traumatic brain injury and neurocognitive impairment. Journal of computer assisted tomography. 2009; 33:293–297. [PubMed: 19346863]

22. Lotocki G, de Rivero Vaccari JP, Perez ER, Sanchez-Molano J, Furones-Alonso O, Bramlett HM, Dietrich WD. Alterations in blood-brain barrier permeability to large and small molecules and leukocyte accumulation after traumatic brain injury: effects of post-traumatic hypothermia. J Neurotrauma. 2009; 26:1123–1134. [PubMed: 19558276]

23. Lowenstein DH. Epilepsy after head injury: an overview. Epilepsia. 2009; 50(Suppl 2):4–9. [PubMed: 19187288]

24. McDonald JW, Stefovska VG, Liu XZ, Shin H, Liu S, Choi DW. Neurotrophin potentiation of iron-induced spinal cord injury. Neuroscience. 2002; 115:931–939. [PubMed: 12435430]

25. Narayan RK, Michel ME, Ansell B, Baethmann A, Biegon A, Bracken MB, Bullock MR, Choi SC, Clifton GL, Contant CF, Coplin WM, Dietrich WD, Ghajar J, Grady SM, Grossman RG, Hall ED, Heetderks W, Hovda DA, Jallo J, Katz RL, Knoller N, Kochanek PM, Maas AI, Majde J, Marion DW, Marmarou A, Marshall LF, McIntosh TK, Miller E, Mohberg N, Muizelaar JP, Pitts LH, Quinn P, Riesenfeld G, Robertson CS, Strauss KI, Teasdale G, Temkin N, Tuma R, Wade C, Walker MD, Weinrich M, Whyte J, Wilberger J, Young AB, Yurkewicz L. Clinical trials in head injury. J Neurotrauma. 2002; 19:503–557. [PubMed: 12042091]

26. Pierce JE, Smith DH, Trojanowski JQ, McIntosh TK. Enduring cognitive, neurobehavioral and histopathological changes persist for up to one year following severe experimental brain injury in rats. Neuroscience. 1998; 87:359–369. [PubMed: 9740398]

27. Pierce JE, Trojanowski JQ, Graham DI, Smith DH, McIntosh TK. Immunohistochemical characterization of alterations in the distribution of amyloid precursor proteins and beta-amyloid peptide after experimental brain injury in the rat. J Neurosci. 1996; 16:1083–1090. [PubMed: 8558237]

28. Povlishock JT, Christman CW. The pathobiology of traumatically induced axonal injury in animals and humans: a review of current thoughts. J Neurotrauma. 1995; 12:555–564. [PubMed: 8683606]

29. Raghupathi R, Conti AC, Graham DI, Krajewski S, Reed JC, Grady MS, Trojanowski JQ, McIntosh TK. Mild traumatic brain injury induces apoptotic cell death in the cortex that is preceded by decreases in cellular Bcl-2 immunoreactivity. Neuroscience. 2002; 110:605–616. [PubMed: 11934469]

30. Salter MG, Fern R. NMDA receptors are expressed in developing oligodendrocyte processes and mediate injury. Nature. 2005; 438:1167–1171. [PubMed: 16372012]
31. Schulz R, Vogel T, Dressel R, Krieglstein K. TGF-beta superfamily members, ActivinA and TGF-beta1, induce apoptosis in oligodendrocytes by different pathways. Cell Tissue Res. 2008; 334:327–338. [PubMed: 19002501]
32. Shaw K, MacKinnon MA, Raghupathi R, Saatman KE, McLntosh TK, Graham DI. TUNEL-positive staining in white and grey matter after fatal head injury in man. Clin Neuropathol. 2001; 20:106–112. [PubMed: 11430493]
33. Suzuki T, Bramlett HM, Ruenes G, Dietrich WD. The effects of early post-traumatic hyperthermia in female and ovariectomized rats. J Neurotrauma. 2004; 21:842–853. [PubMed: 15307897]

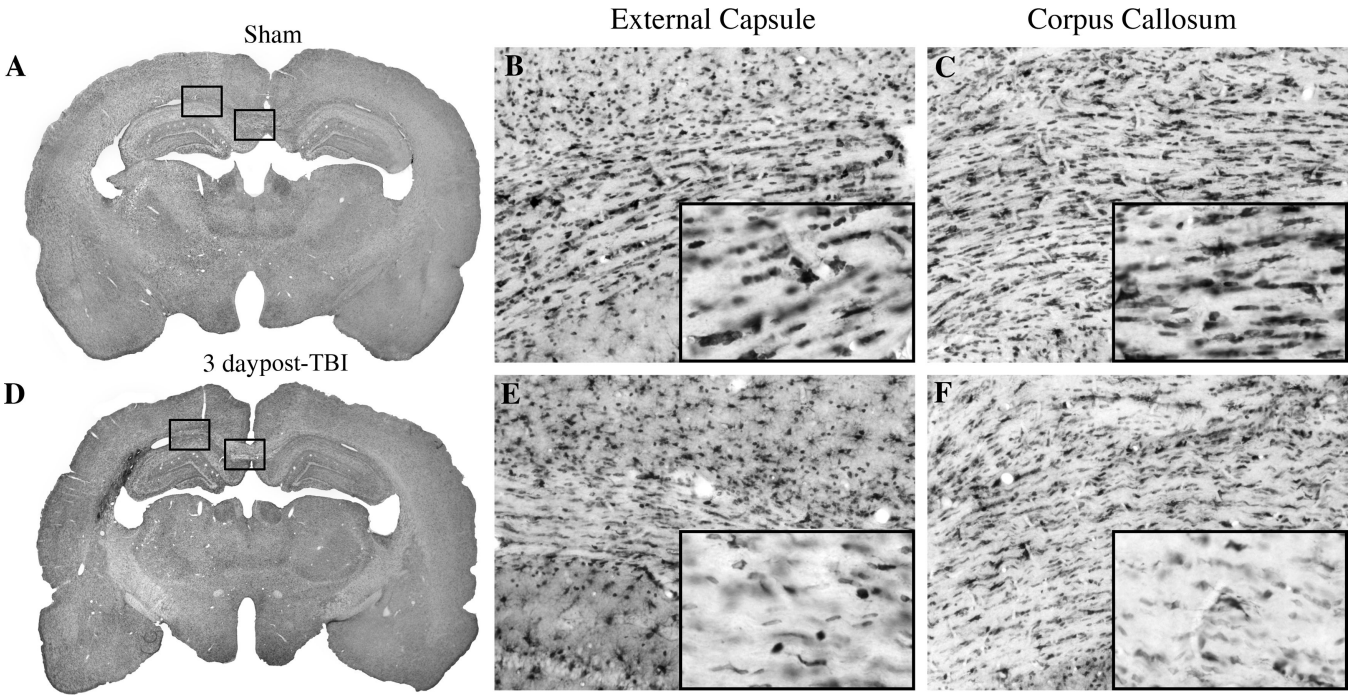

Figure 1.
Micrographs of CC1 immunoreactive oligodendrocytes. Sham (A) animal exhibiting robust staining of CC1 positive cells in the external capsule (B) and corpus callosum (C). In contrast, at 3 days post-TBI animal (D) shows reduced numbers of CC1 positive cells in the external capsule (E) and corpus callosum (F). Magnification 1X (A,D), 10X (B, C, E, F), inset of B, C, E, F (20X).

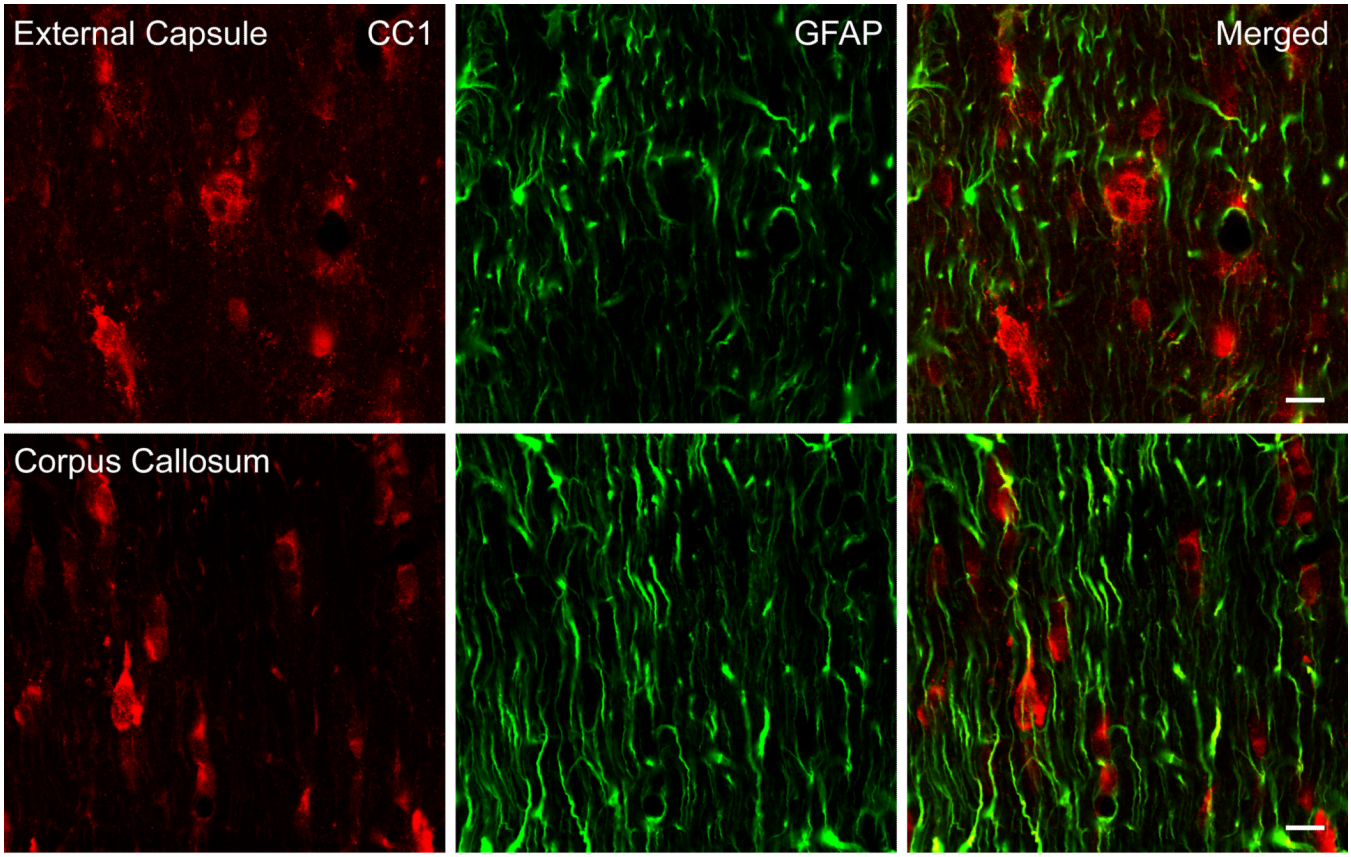

Figure 2.
Confocal micrographs of representative double-labeled CC1 and GFAP immunoreactive cells. CC1 (red) and GFAP (green) positive cells in the external capsule (Row 1) and corpus callosum (Row 2) were investigated in traumatized rats 7 days post injury. CC1 and GFAP colocalization was not observed in these regions of the rat brain (Merged). Bar = 10 microns.

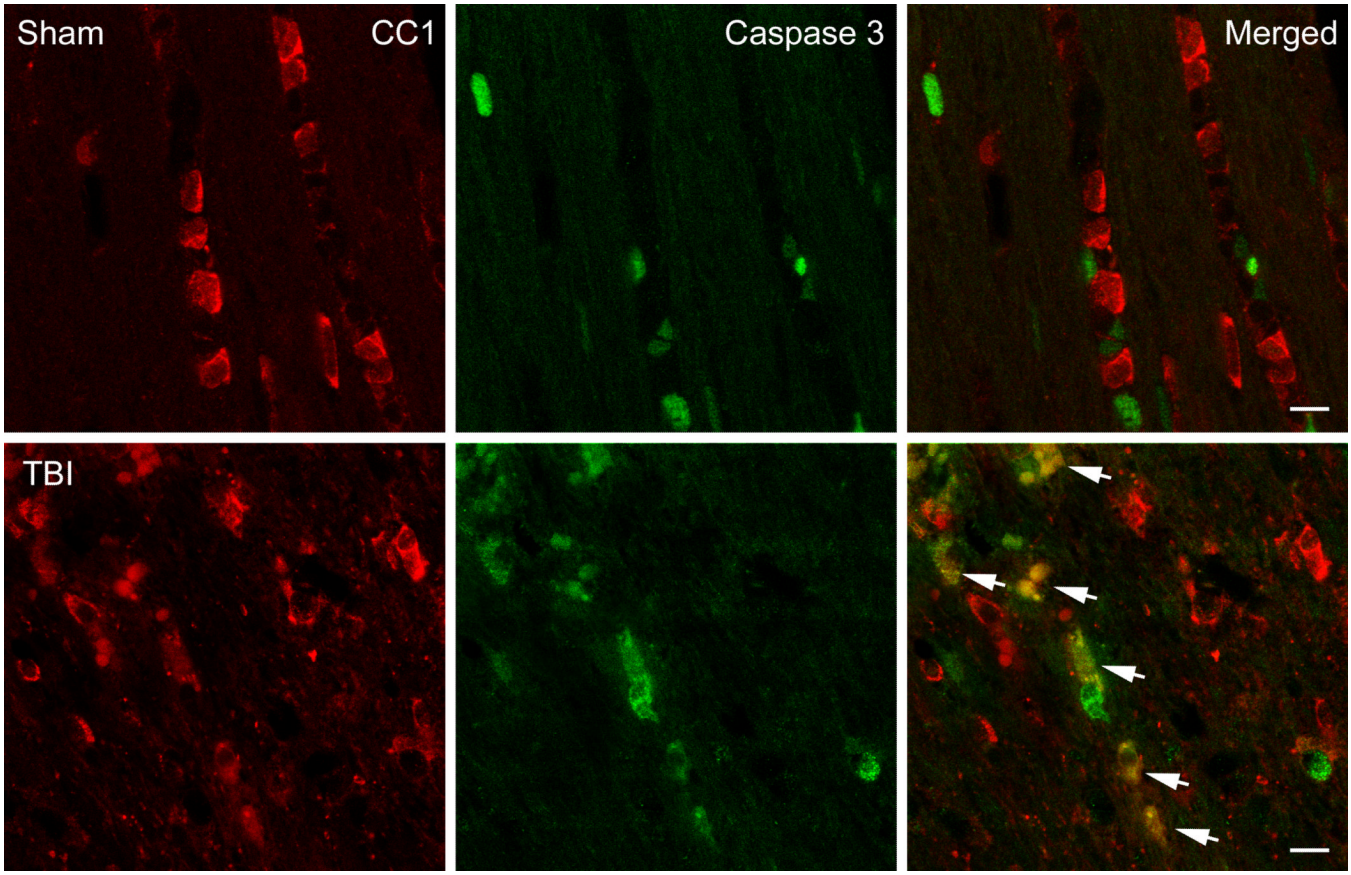

Figure 3.
Confocal micrographs of representative double-labeled CC1 (red)/Caspase 3 (green) positive cells in the external capsule. Sham animals showed CC1 positive cells with no Caspase 3 positive cells (Row 1). In contrast, a 3 day TBI animal demonstrates robust double-labeling (merged) of Caspase 3 and CC1 indicating apoptotic cell death of these oligodendrocyte (Row 2, arrows). Bar = 10 microns.

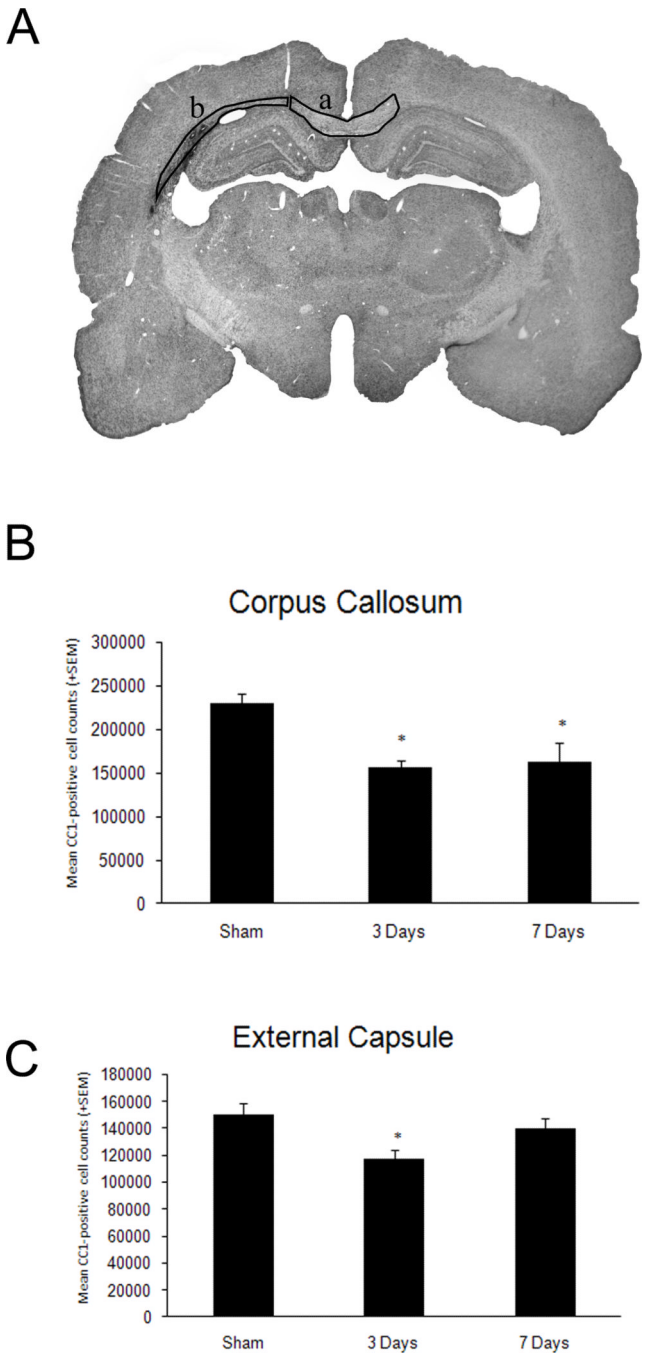

Figure 4.

Quantitative assessment of CC1 positive cells within vulnerable white matter regions. A. Representative micrograph indicating where the stereological cell counts were conducted, corpus callosum (a) and external capsule (b). B. T-test was significant ($p<0.001$) for both time points compared to sham in the corpus callosum. Both 3 and 7 day TBI animals showed significant (*$p<0.001$) reductions in CC1 positive cells compared to sham. C. T-test was significant (*$p<0.02$) for the 3 day TBI group compared to sham in the external capsule. These data demonstrate a reduction in the number of CC1 positive cells in the 3 day TBI group compared to sham.